Diffusively-driven overturning of a stable density gradient

Andrew F. Thompson

1 Introduction

Oceanographic observations from CTD (conductivity, temperature and depth) casts have shown that rapid reversals in the gradient of temperature and salinity with depth is a common feature in many areas, especially in polar regions [14, 12]. These oscillations in temperature and salinity which are typically on the order of tens of meters are thought to be a signature of horizontal intrusions. These intrusions are often referred to as thermohaline intrusions because they are driven by processes related to the different diffusing properties of heat and salt, or what is commonly known as double diffusion.

Double diffusion can occur when two components contribute to the density of a fluid (such as heat and salt in the ocean), but they diffuse at different rates. Double diffusive convection refers to the case when one of the components is stably stratified, the second component is stratified in a destabilizing sense, but the fluid is overall stably stratified. Double diffusive convection is the process by which potential energy stored in the destabilizing component is released. There are two possible configurations for double diffusion at an interface between two fluids. If the slower diffusing component is destabilizing, this is known as a fingering interface and if the faster diffusing component is destabilizing this is known as a diffusive interface. A complete review of double diffusion can be found in the seminal work on buoyancy effects in fluids by Turner [13] and a discussion of double diffusive processes important in the ocean can be found in the review by Schmitt [9].

To understand how double diffusion can generate thermohaline intrusions first consider lateral, density-compensating gradients of temperature and salinity and a vertical stratification that supports salt fingering for example. If this basic state is then perturbed by alternating shear zones, the lateral gradients will create alternating regions where the salt fingers are strengthened (when greater concentrations of salt run over colder water) and weakened (when colder water is over salty water). Since fingering leads to a downward density flux, the regions above increased fingering (the warm salty water) become lighter. If there is some initial slope to the sheared perturbations the warm salty water will continue to rise and propagate, while the cold fresh regions will sink while propagating in the opposite direction. A schematic of this model, which was first explained by Stern [11] and reviewed recently by Ruddick and Kerr [6], appears in figure 1.

While the model described above assumes that the vertical density gradient is initially stratified in a fingering sense, there have been observations of intrusion formation in regions where the ocean is stably stratified in both temperature and salinity [12]. This raises the

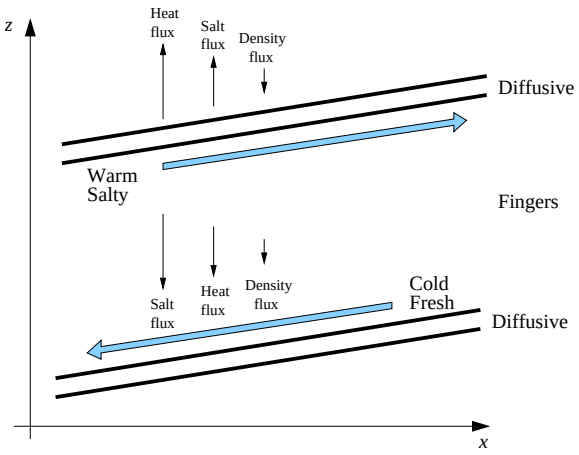

Figure 1: Schematic diagram of a thermohaline intrusion [6]. In the fingering region between the two diffusive interfaces, the downward density flux causes the warm, salty fluid to rise as it propagates to the right, while the cold, fresh fluid becomes denser and sinks.

question of how thermohaline intrusions can form in the lack of a vertical stratification that supports double diffusion.

The aim of this project is to present a model for intrusion formation driven by vertical diffusion in a layer of constant density, but lateral gradients of two diffusing components. The layer sits above a reservoir that has higher concentrations in both components so that the system is stably stratified in both components. In section 2 we briefly discuss previous laboratory experiments that have considered similar problems. In section 3 and 4 we describe the experiments carried out over the summer and our observations. In section 5 we present a simple model of how density and the intrusion lengths evolve. Section 6 contains results from our experiments and a discussion of how they compare to the theory, and we finish with some conclusions and suggestions for future work in section 7.

2 Previous Experiments

There has been a number of previous studies considering laboratory models of intrusion formation in double diffusive systems. All of the models discussed here use a sugar–salt system as opposed to a heat–salt system. This is a common practice in laboratory work because of the complications that arise due to heat losses through the walls of the experimental tank. For this same reason we also use a sugar–salt system in the experiments to be described below. It should be noted that while heat diffuses 100 times faster than salt, in the sugar–salt system, salt diffuses only three times as fast as sugar. Traditionally T (here, salt) refers to the faster diffusing component and S (here, sugar) refers to the slower diffusing component.

Ruddick and Turner [8] in a study familiarly known as the "Christmas tree experiment," first looked at horizontal intrusions from a stable density gradient. They filled the left and right hand sides of a divided tank with a stably stratified sugar and salt solution respectively. The stratifications were set up so that there were no horizontal density gradients anywhere.

At the start of the experiment the barrier was removed which created perturbations that allowed both fingering and diffusive interfaces to form. The study found that fingering dominated the vertical fluxes; sugary intrusions, which lost density through sugar fingers, rose as they propagated to the right, while salty intrusions fell as they propagated to the left. A series of intrusions formed in the tank, the height of which was determined by the initial density stratification. Ruddick, Phillips and Turner [1] returned to these experiments and completed a more thorough study that included theories for the propagation speed of the noses and overturning circulations that occur within each intrusion.

Noting similarities between thermohaline intrusions and gravity currents, Maxworthy [5] completed an experimental study on double diffusive gravity currents. He considered both the release of a fixed volume of fluid and a constant inflow for both diffusive and fingering interfaces. Maxworthy found that horizontal momentum could be transferred across the interface of the current and in many cases this transfer dominated the viscous forces more commonly associated with gravity currents. This process was modeled as a double diffusive retarding force that depended on both the horizontal velocity of the current and a vertical velocity defined by the ratio of the vertical flux to the vertical density gradient of the more rapidly transferred component (S for a fingering interface and T for a diffusive interface).

Yoshida, Nagashima and Ma [4] later used this double diffusive retarding force to help explain their observations of double diffusive lock exchange experiments. The experiments considered homogeneous solutions of sugar and salt separated by a barrier. A slight density difference between the two sides of the tank determined whether the sugar solution ran under the salt solution and generated a diffusive interface or alternatively the sugar solution ran over the salt solution and formed a fingering interface. Yoshida *et al.* found that the length of the intrusions grew linearly with time, and they developed a simple theory to explain this linear relationship.

3 Experimental Procedure

Before each experiment four solutions, corresponding to the four regions marked in figure 2, were prepared using distilled water, pure cane sugar (obtained from a grocery store) and kosher salt. Solutions 1 and 2 had a density of approximately 1.02 g/cm^3, but contained different concentrations of sugar and salt. In one configuration the contribution of sugar to the density of solution 1 was twice that of salt, while in solution 2, the contribution of salt to the density was twice that of sugar. In the second configuration, solution 1 contained only sugar and solution 2 contained only salt. In all experiments solution 1 was dyed blue. By diluting with distilled water, the densities of these two upper layers were set equal to $\pm 5 \times 10^{-6}$ g/cm^3 using an Anton Paar precision densitometer. Solution 3, composed of both salt and sugar, had a density of 1.05 g/cm^3 with the same concentration of salt as solution 2. Finally solution 4 had a density of 1.065 g/cm^3 with again the same salt concentration as solutions 2 and 3. The appropriate quantities of salt and sugar necessary to create these solutions were determined from Ruddick and Shirtcliffe [7]. The solutions were allowed to sit overnight to achieve room temperature. This minimized the effects of temperature fluctuations and heat diffusion in the experiments.

The experiments were conducted in a Perspex tank 60 cm long, 20 cm deep and 10 cm wide. The tank was fitted with a lock gate that could be raised to any height and fixed in

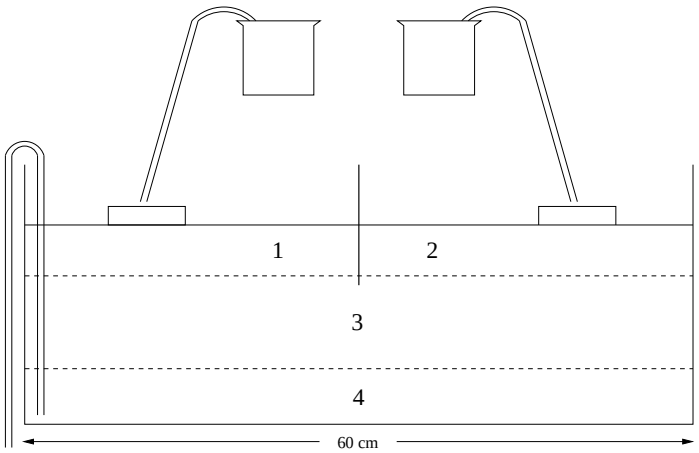

Figure 2: Diagram of laboratory equipment. Solutions 1 and 2 have the same density, but are composed of different concentrations of sugar and salt. The density due to sugar is larger in solution 1 than solution 2. Solution 3 is denser than 1 and 2, but contains the same amount of salt as solution 2. Solution 4 is denser than solution 3, but again contains the same amount of salt as 2 and 3. A barrier separates solutions 1 and 2 before the start of the experiment and fluid from region 4 is removed with a siphon to lower the surface and initiate the experiment.

place with a small clamp. This gate was used to separate solutions 1 and 2 until the start of the experiment. The different solutions were layed down in the tank as depicted in figure 2. The fluid was poured through siphons at a flow rate of approximately 3 mL/s onto sponges floating on the surface in order to minimize mixing. The thickness of the upper layer was varied in each experiment; layers 3 and 4 were generally 1.5 to 2 cm thicker than the upper layer.

The experiments were initiated using a new method for lock release. In similar experiments the barrier is removed by manually or mechanically pulling it out of the tank. Here we removed water from layer 4 by use of a siphon. This lowered the surface of the entire system at a slow rate until the surface was entirely below the barrier.

After initiation, measurements were made using a number of visualization techniques including shadowgraphs, still photography and time-lapse video. Measurements were made of the propagation of the intrusions as they formed. Flow visualization was also aided by dropping potassium permanganate crystals in the flow at different times during the experiment. Samples were removed at various locations and times using a syringe and density measurements were made using the precision densitometer.

Parameters varied in the system were the initial thickness of the upper layer, and the variation in properties across the barrier in the upper layer. These parameters are listed in table 1, where configuration 1 refers to mixed solutions in the upper layer and configuration 2 refers to pure sugar/pure salt solutions in the upper layer.

Experiment Number	Configuration	Initial upper layer depth h_0 (cm)
14	1	1.5
12	1	1.8
15	1	2.0
17	1	2.2
9	1	2.5
16	1	4.8
8	1	8.0
19	2	1.2
21	2	1.3
18	2	1.8
26	2	2.0
22	2	2.5
25	2	3.0
24	2	5.0
27	2	2.5

Table 1: Parameters varied in the experiments. Configuration 1 refers to mixed solutions where sugar contributes twice as much as salt to the density on the left hand side of the barrier, and salt contributes twice as much as sugar to the density on the right hand side. Configuration 2 refers to a pure sugar solution on the left hand side and pure salt solution on the right hand side. Experiment 27 was carried out to measure density as a function of time.

4 Observations

4.1 Initiation

As soon as the sugary upper layer solution was added to the top layer, salt began to diffuse upward from the reservoir below. Since the salty layer had the same salt concentration as the reservoir no salt diffused upward. Therefore, the bottom of the sugary layer became more denser than the salty layer. As fluid was siphoned out of the lowermost layer, the right and left sides of the upper layer came into contact at time $t = 0$. Observations showed that the densities could be calibrated such that in most experiments there was a period of five to ten seconds where neither fluid showed a net propagation into the opposite region. This was then followed by a slight intrusion of sugary fluid (dyed blue) toward the right. The shape of this intrusion was a very thin wedge with no turbulent motions apparent near the nose. This intrusion of sugary fluid in turn induced a return flow into the left hand side simply by mass conservation. Figure 3*a* shows a photograph of an experiment after these initial intrusions.

Since salty fluid pushed into a region with sugary fluid above, sugar fingers formed that vigorously mixed the region to the left of the barrier (figure 3*b*). This caused fluid depleted of sugar to become buoyant, rise and pool at the surface to the left of the rising barrier. Once reaching the surface the lighter fluid began to propagate to the left into the sugary region while remaining at the surface.

While vigorous convection characterized the initiation of this experiment, the turbulent nature of the flow quickly resolved itself into a sharp diagonal interface that linked the leftward moving upper intrusion and the rightward moving lower intrusion (figure 3*c*). Despite the vigorous convection, there still seemed to be minimal mixing of salty and sugary fluid as evidenced by the lack of mixing of the blue dye. Once this interface formed, strong convective plumes were observed both above and below the interface. In general, the greater the depth of the upper layer and the larger the salt and sugar contrast across the barrier the stronger the convective plumes appeared to be.

4.2 Intrusion shape

As the lower, sugary intrusion received salt from both the lower reservoir and the fluid above, it continued to become denser and propagated to the right along the interface between the upper layer and the reservoir (figure 4). The current intruded as a wedge and did not exhibit the turbulent head common to gravity currents in a homogeneous ambient. The flow of the current was on the order of 1 cm/min, but seemed to depend strongly on the depth of the upper layer. The interface between the dyed lower intrusion and the clear upper intrusion appeared to be a straight line connecting the fronts, with some small curvature at the noses.

The current propagating to the left at the surface seemed to move at a nearly constant velocity that was also dependent on the height of the upper layer. In all experiments the leftward moving intrusion hit the end wall first and generally did not seem to slow upon nearing the end wall. The rightward moving lower intrusion did slow upon nearing the end wall.

In all the experiments with a small aspect ratio, only two layers were observed to form in the upper region with the clear, salty layer running over the dyed, sugary layer. The interface

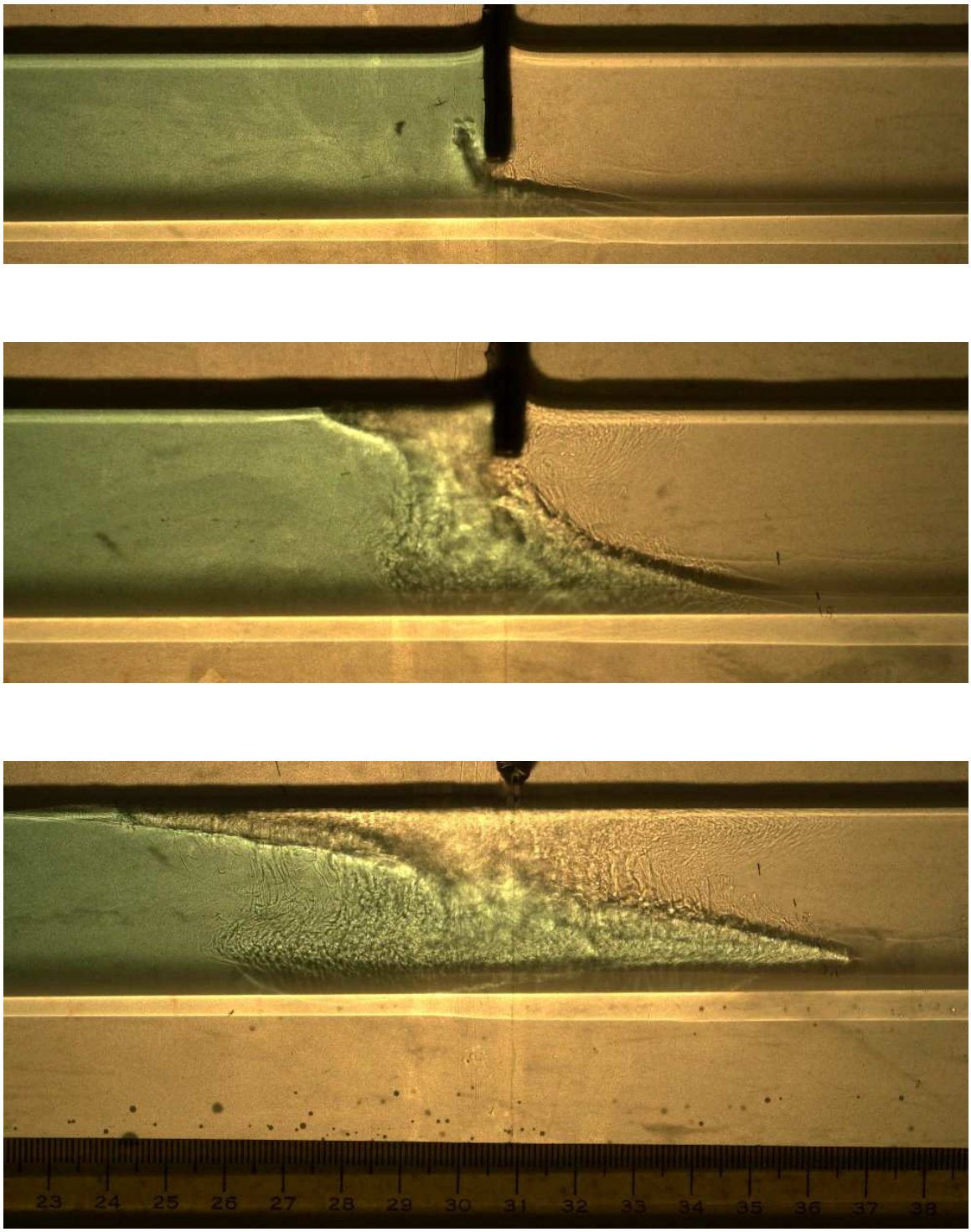

Figure 3: Photographs of initiation of experiment 25 at (*a*) $t = 58$ s, (*b*) $t = 122$ s, (*c*) $t = 184$ s.

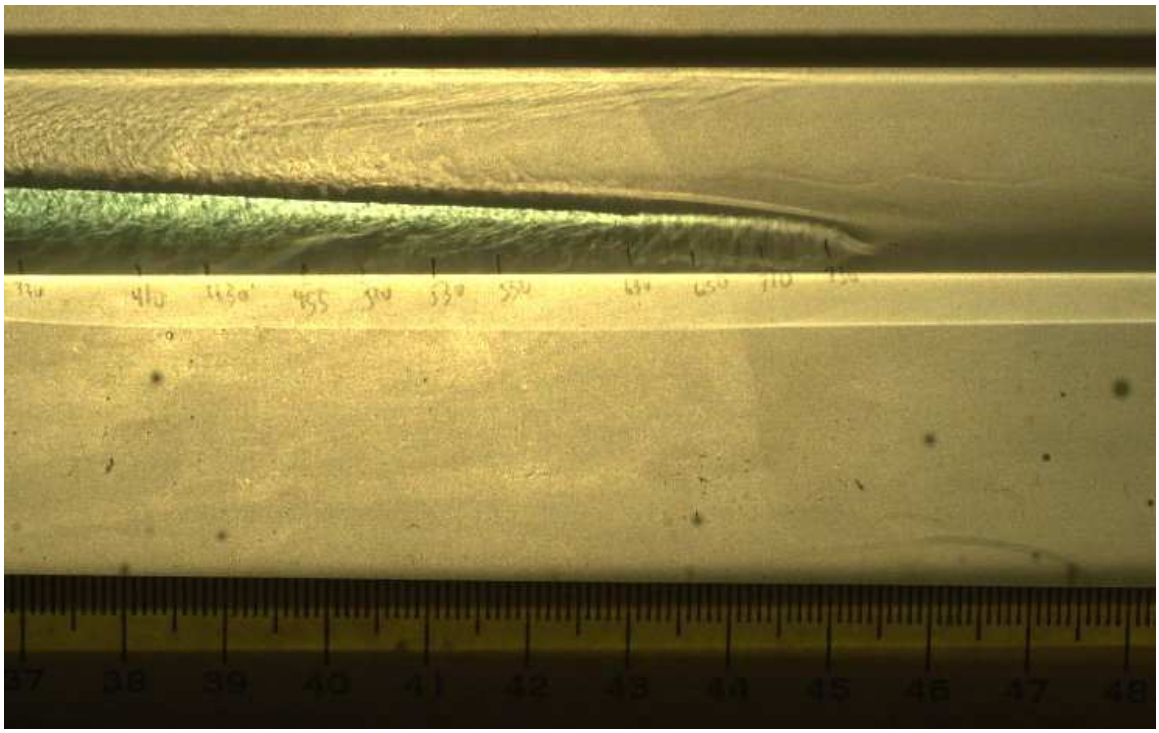

Figure 4: Photograph of right-moving lower intrusion from experiment 25 at t = 10:50.

between these two regions remained sharp throughout the experiment until convection ran down and diffusion started to thicken the interface slowly. Convection lasted for most of the experiment although it weakened steadily throughout. The convective motions appeared to have a vertical length-scale, which was most likely determined by the shear in the two layers discussed below. Convection was not observed in a region extending a centimeter or two behind the head of the current (figure 4). It is possible that this length-scale is related to the diffusivity of the salt and the velocity of the nose.

4.3 Velocity structure

Besides the leftward and rightward propagation of the upper and lower intrusions respectively, there was also an overturning circulation within each layer. The sense of this circulation was clockwise in both layers and in general the velocities were greater than those of the intrusions. This feature was observed and commented upon by Ruddick *et al.* [1]. Visualization with the use of dye crystals showed strong shear occurred along the interface between the two regions of fluid as the horizontal velocity is to the left (up slope) in the upper layer and to the right (down slope) in the lower layer. Return flows were to the right near the surface in the upper layer and to the left near the interface with the reservoir in the lower layer. Observations also seemed to indicate regions of high shear both near the surface and at the interface between the upper layer and reservoir. Dye crystals that fell through the upper layer showed that velocities in the lower reservoir were very small compared to the velocities in the upper layer. While we expect no net transport over the entire height

of the upper layer, there was a net transport of fluid to the left in the clear layer and a net transport to the right in the blue-dyed layer since the sloped interface continued to flatten until it appeared horizontal.

5 Some Simple Theory

5.1 Initiation

We begin this section by writing down the governing equations for our experiment. We assume a two-dimensional, incompressible, Boussinesq salt and sugar system (T and S respectively). The equations of motion are given by

$$\xi_t + J(\psi, \xi) = -g\left(\alpha T_x + \beta S_x\right) + \nu \nabla^2 \xi, \tag{1}$$

$$T_t + J(\psi, T) = \kappa_T \nabla^2 T, \tag{2}$$

$$S_t + J(\psi, S) = \kappa_S \nabla^2 S, \tag{3}$$

$$w = \psi_x, \quad u = -\psi_z, \quad \xi = \nabla^2 \psi, \tag{4}$$

$$\rho = \rho_0 \left(1 + \alpha T + \beta S\right) \tag{5}$$

where

$$\alpha = \frac{1}{\rho_0}\frac{\partial \rho}{\partial T}, \qquad \beta = \frac{1}{\rho_0}\frac{\partial \rho}{\partial S} \tag{6}$$

are the coefficients of expansion of salt and sugar respectively and J represents the Jacobian. These equations represent the curl of the horizontal and vertical momentum equations, conservation of salt, conservation of sugar and conservation of mass. It is quickly apparent from these equations that it would be difficult to solve these equations analytically, and even numerically it would be a non-trivial task. Therefore, in the scope of this project we have attempted to understand parts of the problem rather than a complete solution.

We first considered the initiation of the experiment by assuming that the barrier is removed instantaneously without any disturbances at time $t = 0$. Because of the differences in diffusion rates, we expect that at early times we can neglect the effects of sugar diffusion.

A simple problem is to consider the horizontal diffusion of salt across the vertical interface separating the two regions in the upper layer. At early times we assume the non-linear terms in the governing equations above are small and that across the front $\partial_x \gg \partial_z$. We simply solve the diffusion equation,

$$T_t = \kappa_T T_{xx} \tag{7}$$

with the boundary conditions $T \to 0$ as $x \to -\infty$ and $T \to \Delta T_0$ as $x \to +\infty$. Solving these equations gives us a solution in terms of the error function, but we will choose to solve the diffusion equation using Laplace transforms so we can use the solution in the momentum equation as well. After taking the Laplace transform of equation 7 and the boundary conditions we find the solution in Laplace space is given by

$$\tilde{T} = \frac{\Delta T_0}{2s}\left(2 - \exp\left[-\sqrt{\frac{s}{\kappa_T}}x\right]\right) \qquad x > 0 \tag{8}$$

$$\tilde{T} = \frac{\Delta T_0}{2s}\exp\left[\sqrt{\frac{s}{\kappa_T}}x\right] \qquad x < 0. \tag{9}$$

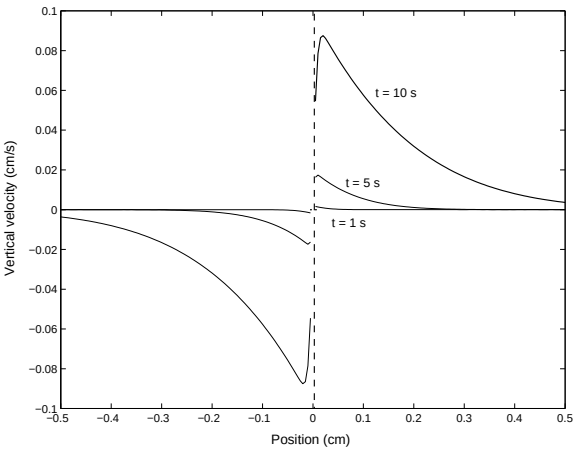

Figure 5: Plot of vertical velocity as a function of position from the vertical interface at various times caused by horizontal diffusion of salt.

Neglecting the nonlinear terms in the curl of the momentum equation and dropping derivatives with respect to z we seek to solve,

$$\psi_{xxt} = -g\alpha T_x + \nu\psi_{xxxx}. \tag{10}$$

Again we proceed by taking the Laplace transform of this equation, and apply the expressions for $\tilde{T}$ that we found above. We can solve this equation for $\tilde{\psi}_{xx}$ and integrate once with respect to x. We then transform back to the time domain using the convolution theorem to find ψ_x or

$$w = \frac{g\alpha\Delta T_0}{2\nu}\left(\frac{1}{\nu} - \frac{1}{\kappa_T}\right)^{-1}\left(\int_0^t \left[\operatorname{erfc}(\eta_\kappa) - \operatorname{erfc}(\eta_\nu)\right] du\right), \qquad x > 0, \tag{11}$$

where $\eta_\kappa = x/2\sqrt{\kappa_T u}$ and $\eta_\nu = x/2\sqrt{\nu u}$. Using the same procedure we can find the vertical velocity for $x < 0$, and find that it is just the opposite of the expression given above. A plot of the vertical velocity as a function of distance from the interface at various times using parameters typical from our experiments is shown in figure 5. As we expect, salt diffuses horizontally from positive to negative x generating a larger density that drives a downward flow for $x < 0$ and reducing the density and driving an upward flow for $x > 0$. This seems to indicate that an instability could occur even without the lower reservoir. We expect the reservoir has a much larger effect, though, and we are planning further experiments to test this more thoroughly.

We next consider diffusion of salt across the horizontal interface between the dense lower reservoir and the sugar solution in the upper layer. Once again we will neglect the effects of sugar diffusion and only consider vertical derivatives since they are much larger than the horizontal derivatives at early times. We consider the diffusion equation

$$T_t = \kappa_T T_{zz}, \tag{12}$$

which we can solve in terms of an error function and then use to express the density in the

upper layer as a function of vertical position and time. Using equation 5,

$$\rho = \rho_0 \left(1 + \alpha \Delta T_0 + \frac{\alpha \Delta T_0}{2} \mathrm{erfc}(\eta_z)\right), \tag{13}$$

where $\eta_z = z/2\sqrt{\kappa_T t}$, and ΔT_0 is the initial salinity difference across the interface.

As a simple analysis at this point, we can argue that the region that gained density due to diffusion will intrude into the salty fluid as a gravity current. We can estimate the increase in density due to diffusion by taking the mean density increase across the diffusive boundary layer $\sqrt{\kappa_T t}$. Rather than integrating (13), we can take the density gradient as linear to leading order to find that the mean density change is given by

$$\Delta \rho = \frac{\rho_0 \alpha \Delta T}{4}. \tag{14}$$

A gravity current is characterized by the Froude number, $\mathrm{Fr} = u/\sqrt{g'h}$. Here $g' = g\Delta\rho/\rho_0$ is the reduced gravity and we take the length scale h to be the diffusive length scale $\sqrt{\kappa_T t}$. Typically $Fr = 1$ at the nose of a gravity current. Considering times less than one minute, $t \sim O(10)$, we find that $u \approx 0.5$ cm/s. Although this represents an extremely thin layer of fluid, the velocity determined by this simple method is much larger than the velocities observed in the experiments.

One likely reason for the disagreement is that the horizontal interface is not actually sharply defined. In the process of filling the tank, some mixing occurs that leads to a thin region of stratification on both sides of the barrier. This then makes it much more difficult to quantify the rate at which salt diffuses from the reservoir into the upper layer. Ruddick *et al.* [1] found that the velocity of intrusions propagating into a stratified ambient scaled like Nh, where N is the buoyancy frequency. The quantity u/Nh is equivalent to a Froude number, and they also found the velocity was much smaller than expected for gravity current dynamics. Their results showed,

$$u \sim 0.005 Nh. \tag{15}$$

Ruddick *et al.* did not provide an explanation for the small size of the Froude number, and it is a problem that begs further study.

An important quantity in double diffusive convection is the flux ratio γ defined as

$$\gamma = \frac{\beta F_S}{\alpha F_T} \tag{16}$$

for a diffusive interface, and the reciprocal of (16) for a fingering interface (so that γ is always less than 1). Measurements of γ have shown that its value depends on the density ratio, which is given by

$$R_\rho = \frac{\beta \Delta S}{\alpha \Delta T} \tag{17}$$

for a diffusive interface. For $R_\rho > 2$, Turner [13] has found that

$$\gamma = \sqrt{\frac{\kappa_S}{\kappa_T}}. \tag{18}$$

As R_ρ approaches 1, though, the value of γ also approaches 1. Turner interpreted this result by arguing that as R_ρ approaches 1, convection becomes more turbulent and therefore the same processes are transporting both diffusing components and the ratio of the fluxes are approximately equal. At the initiation of our experiments, the value of R_ρ has carefully been set to 1 so that density is compensated across the front. This may indicate that although we observe strong turbulent motions, there may be very little change in density associated with these motions.

5.2 Intrusion propagation

A second approach we have taken to modeling the rightward and leftward moving intrusions is based on the work on Yoshida *et al.* [4]. We assume that after some period of time the vertical interface between the salt solution and sugar solution has tilted so that salty water is riding over fresh. As an initial condition we assume that the density jump across the interface is still zero which may be accurate for early times if the flux ratio γ is close to 1 as discussed above.

We can write that the change in density in the salty solution is due to a flux of salt out of this layer and a flux of sugar into this layer. This can be written as

$$\frac{d\rho_T}{dt} = -\alpha F_T \frac{1-\gamma}{h_0/2}, \tag{19}$$

where ρ_T is the density in the salty layer and h_0 is the initial depth of the upper layer. This model assumes that the layers are well mixed and that the density is a function of time only. The factor of 2 is a geometrical factor included because the current is approximately triangular. We note that this is a simplified model as our measurements have indicated that there are spatial gradients in the density field.

The flux of salt across the interface can be related to the change in the salinity difference across the interface,

$$\alpha F_T = \frac{\rho_0 h_0}{2} \frac{d}{dt} \left(\alpha \Delta T\right). \tag{20}$$

Finally a third equation is needed as a parameterization of the salt flux as a function of the salt gradient. A review of flux laws for double diffusive convection across a diffusive interface is given in Kelley *et al.* [3]. For simplicity we use the flux relationship determined by Turner [13] where he argued that for turbulent convection

$$\alpha F_T = C(\alpha \Delta T)^{4/3}, \tag{21}$$

where C is a dimensional constant that depends on the solution properties and the density ratio R_ρ [10]. It is more difficult to judge the validity of assuming that C is a constant because in the scope of this project we were unable to measure concentrations of salt and sugar separately, and therefore it is difficult to estimate how R_ρ changes over the course of the experiment.

At this point we can use equations (20) and (21) to find an expression for the salt jump across the interface as a function of time,

$$\alpha \Delta T = (\alpha \Delta T_0)(1 + t/\tau)^{-3}, \tag{22}$$

where τ is a time scale given by

$$\tau = \frac{3\rho_0 h_0}{2C(\alpha\Delta T_0)^{1/3}}. \tag{23}$$

Assuming $R_\rho \approx 2$ in determining C, and using parameters from our experiments we find that $\tau = O(10^3\text{s})$. We note here that we expect R_ρ to be small based on the propagation speed of our current (density differences must be small), but there are also large fluctuations in the value of C for $1 < R_\rho < 2$.

Finally we can use equations (21) and (22) to integrate equation (19) with time. From this we obtain

$$\rho_T = \rho_0 \left[1 + \alpha\Delta T_0(1-\gamma)(1+t/\tau)^{-3} + \alpha\Delta T_0\gamma\right]. \tag{24}$$

The density in the lower, sugary layer can be determined in a similar manner and using the fact that $\alpha\Delta T_0 = \beta\Delta S_0$ we find,

$$\rho_S = \rho_0 \left[1 - \alpha\Delta T_0(1-\gamma)(1+t/\tau)^{-3} + \alpha\Delta T_0(2-\gamma)\right]. \tag{25}$$

Combining these two equations then gives us an expression for the density difference across the interface as a function of time,

$$\Delta\rho = 2\rho_0(\alpha\Delta T_0)(1-\gamma)\left(1 - (1+t/\tau)^{-3}\right). \tag{26}$$

We have also analyzed this model for a flux condition that is controlled purely by diffusion. This modification only affects our parameterization of the flux law given in (21), where now the flux of salt across the interface depends on the salinity gradient across the interface. To model this we assumed that there is some length scale h_m associated with the thickness of the interface and that this was maintained at a constant value. We believe that this assumption may be valid while the shear at the interface is high. Then we can write

$$\alpha F_T = \rho_0\kappa_T\frac{\alpha\Delta T}{h_m}. \tag{27}$$

Following the same steps as before we can integrate up equations 20 and 27 to obtain

$$\Delta\rho = 2\rho_0(\alpha\Delta T_0)(1-\gamma)\left(1 - \exp\left[-\kappa t/h_0 h_m\right]\right). \tag{28}$$

Following the work of both Maxworthy [5] and Yoshida *et al.* [4], we now argue that for most of the experiment, the buoyancy force generated by density differences across the interface is balanced by a double diffusive retarding force. This double diffusive force is given in Maxworthy [5] as

$$F_{DD} = \rho UVL, \tag{29}$$

where U and V are defined as

$$U = \frac{L}{t}, \quad \text{and} \quad V = \frac{\alpha F_T}{\rho\alpha\Delta T}. \tag{30}$$

The buoyancy force is given by $F_B = \Delta\rho g h_0^2$, so we can write

$$F_B = 2\rho_0(\alpha\Delta T_0)(1-\gamma)gh_0^2\left[1 - (1+t/\tau)^{-3}\right], \tag{31}$$

$$F_{DD} = C(\alpha\Delta T_0)^{1/3}(1+t/\tau)^{-1}L^2t^{-1}, \tag{32}$$

where we have used the four-thirds flux parameterization as opposed to the diffusive flux parameterization. Equating these two forces we obtain a scaling for L,

$$L \propto (\rho_0 g)^{1/2} (\alpha \Delta T_0)^{1/3} h_0 \sqrt{(1 + t/\tau)\left(1 - (1 + t/\tau)^{-3}\right) t}. \tag{33}$$

We can show that for both $t \ll \tau$ and $t \gg \tau$, $L \propto t$ from the expression above, and even when $t \sim \tau$ the t dependence is well approximated by a linear curve [4].

6 Results

Figures 6 and 7 show measurements of density as a function of position in the tank after the experiment has neared run-down. All measurements were taken between one hour and one and a half hours after the start of the experiment. On the x-axis, 0 cm corresponds to the lefthand wall of the tank and 60 cm corresponds to the right-hand wall. The clear symbols represent measurements taken in the upper layer above the interface between the two fluids and the closed symbols represent measurements taken below this interface. Note that density decreases upward on the y-axis in figures 6, 7, and 8 for easier interpretation of the graph.

Figure 6 shows the density measurements from the experiments that had mixed initial conditions. In these experiments, the density in the upper layer was 1.02 g/cm^3. Sugar contriubted twice as much to the density in the left side and salt twice as much in the right side leading to a property contrast across the barrier, $\alpha \Delta T_0 = \beta \Delta S_0 = 0.0067$. The data show that there is still a small positive horizontal density gradient. This most likely means that the experiment has not fully run down to completion. The jump in density across the interface is roughly 0.002 g/cm^3. Fewer measurements of density were made in the experiments with pure sugar and pure salt initial conditions, figure 7. It is clear, though, that the density jump is considerably larger than in the other experiments. The density difference here is roughly 0.006 g/cm^3 which is three times as large as $\Delta\rho$ in figure 6. This agrees well with our theory that the run-down density jump across the interface should scale linearly with $\alpha \Delta T_0$, since $\alpha \Delta T_0$ is 0.02 in the pure salt/pure sugar configuration, or roughly three times as large as the mixed configuration experiments.

In experiment 27 we took density measurements at various heights and times in the center of the tank. These values appear in figure 8 with the different symbols representing the location at which the sample was taken as described in the key. As expected, density decreased steadily in the upper layer and increased steadily in the lower layer. Measurements made just above and below the interface (regions 2 and 3) seem to reach a quasi-equilibrium state after approximately 20–30 minutes, while measurements taken near the surface and near the reservoir interface reach nearly steady values after an hour or more. These measurements seem to show that despite the convection observed in the experiments, there may be either a staircase or a stratified density profile. The vertical density structure could depend strongly on the overturning circulation that is observed. We further note that the density change at region 4 is the largest because of the continuous diffusion of salt into this region from the lower reservoir.

From equations (26) and (28) we can see that the run-down time for the density jump across the interface is τ or $h_0 h_m / \kappa_T$ for the four-thirds flux law or the diffusive flux law

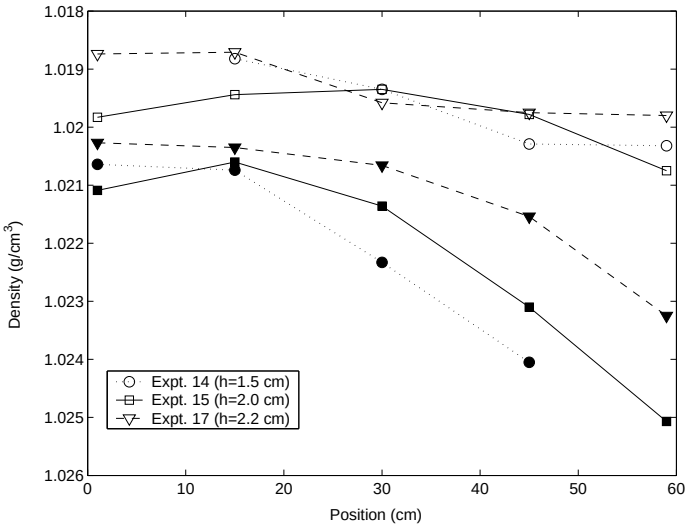

Figure 6: Density in the upper layer as a function of position in the tank after run-down (between 60 and 80 minutes after initiation) for mixed solution initial conditions. The open symbols correspond to measurements taken above the interface and closed symbols to measurements taken below the interface. Density decreases along the y-axis.

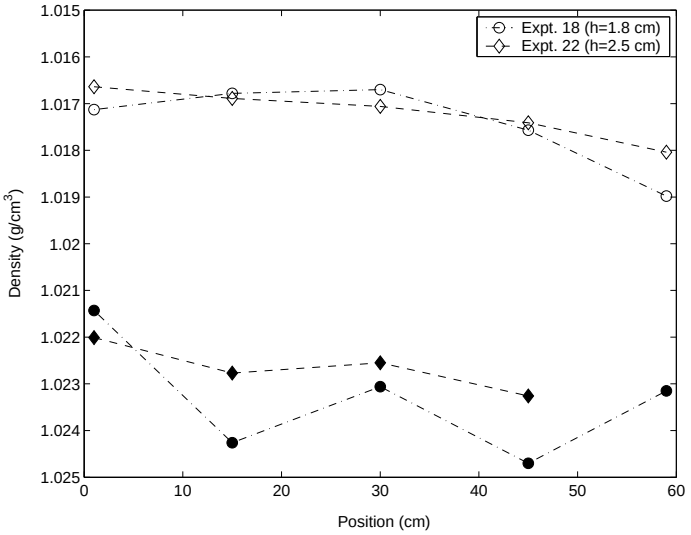

Figure 7: Density in the upper layer as a function of position in the tank after run-down (between 60 and 80 minutes after initiation) for pure salt/pure sugar initial conditions. The open symbols correspond to measurements taken above the interface and closed symbols to measurements taken below the interface. Density decreases along the y-axis.

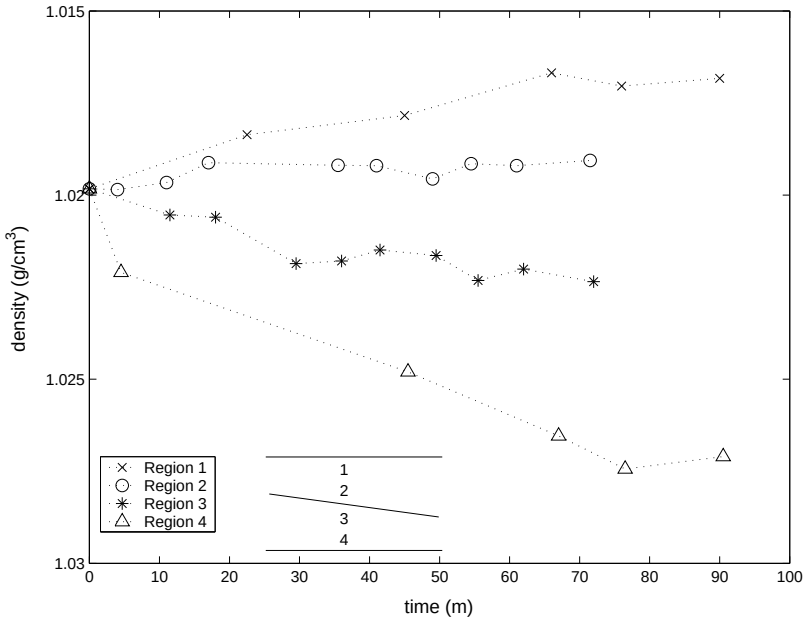

Figure 8: Density measurements as a function of time from experiment 27. The symbols refer to different heights where samples were removed as indicated in the key above. All samples were removed from the center of the tank.

respectively. As given earlier, $\tau \sim 10^3$ s and

$$\frac{h_0 h_m}{\kappa_T} \sim \frac{1\text{cm}(.05\text{cm})}{1 \times 10^{-5}\text{cm/s}^2} \sim 5 \times 10^3\text{s}. \tag{34}$$

Figure 8 may then indicate that the four-thirds law is a decent approximation close to the interface, but the assumption that both layers are well-mixed is certainly not valid. Also, after run-down, we expect $\Delta\rho \approx 2\rho_0(\alpha\Delta T)(1-\gamma)$. For a diffusive interface and $R_\rho > 2$, Turner [13] gives $\gamma = 0.577$ for a one-dimensional salt–sugar system. Therefore we expect $\Delta\rho \approx 0.87\rho_0(\alpha\Delta T)$ or 0.0174 g/cm^3 for the pure salt/pure sugar intitial conditions. Our measurements show that the density difference is smaller than this estimate by a factor of 2 or 3. This may be explained by the fact that at least at the initiation of our experiment, $R_\rho = 1$ and as R_ρ approaches 1, γ also approaches 1. Furthermore, our system is two-dimensional, while Turner's value for γ was derived from a one-dimensional system.

Figures 9 and 10 show measurements of the front position of the upper and lower intrusions respectively as a function of time from the experiments with pure salt/pure sugar initial conditions. The various symbols represent different initial thicknesses h_0. From both figures it is clear that the intrusion velocity depends strongly on the layer depth. Both figures have log-log axes and various power law relations are shown with dashed lines for reference. The length of the upper intrusion seems to depend linearly on time, so that the velocity is constant. There are no pronounced end wall effects, although there may be some late-time behaviour and a change in regime for the slowest experiment where $h_0 = 1.2$ cm. Most of the measurements of the lower intrusions seem to indicate that the velocity is approximately constant, although there does seem to be a monotonic increase in slope

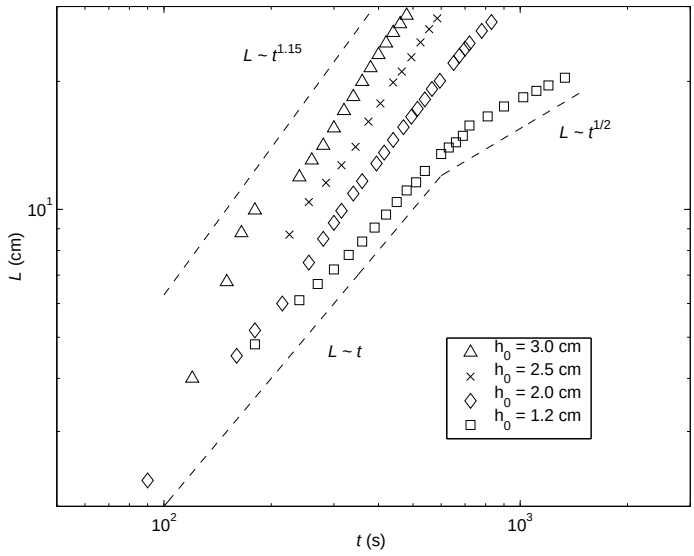

Figure 9: Position of upper intrusion fronts as a function of time for pure salt/pure sugar initial conditions. Power law relations are shown with dashed lines for reference.

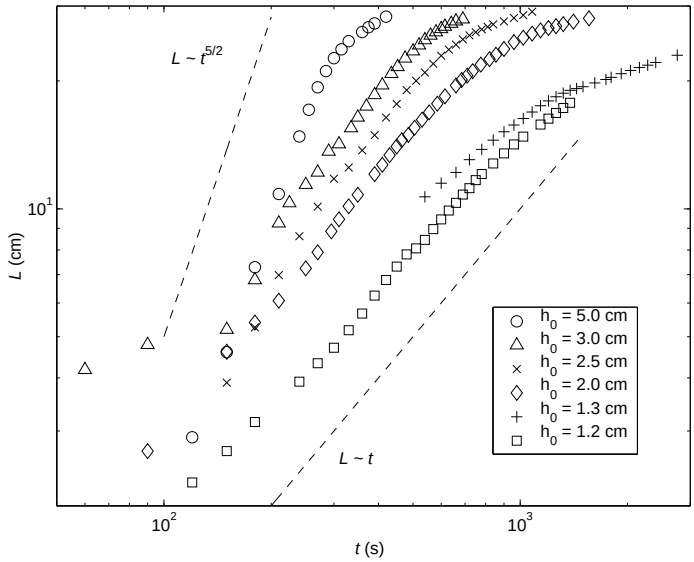

Figure 10: Position of lower intrusion fronts as a function of time for pure salt/pure sugar initial conditions. Power law relations are shown with dashed lines for reference.

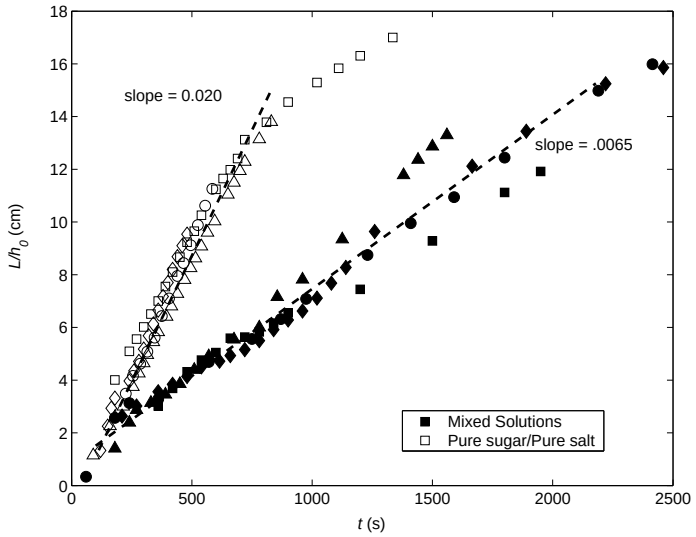

Figure 11: Position of upper intrusion fronts non-dimensionalized with respect to upper layer thickness. Open symbols refer to pure salt/pure sugar initial conditions, closed symbols refer to mixed solutions initial conditions.

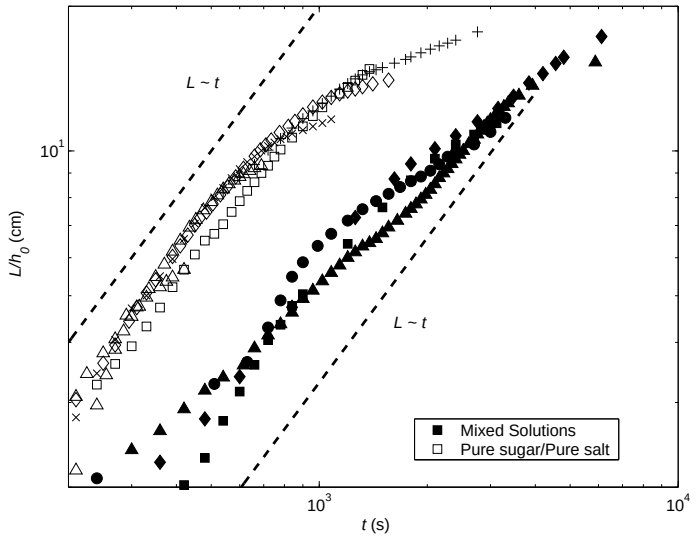

Figure 12: Position of lower intrusion fronts non-dimensionalized with respect to upper layer thickness. Open symbols refer to pure salt/pure sugar initial conditions, closed symbols refer to mixed solutions initial conditions.

in figure 10 with increasing layer depth. For a very deep upper layer, $h_0 = 5.0$ cm, the velocity increases with time with $L \sim t^{5/2}$ or $U \sim t^{3/2}$. There is a much more pronounced end wall effect in the lower layer intrusion due to stratification that arises at the upper layer–reservoir interface when filling the tank. This leads to a blocking flow, which feels the presence of the end wall much earlier than the upper intrusion [2].

Finally, in figures 11 and 12 we have non-dimensionalized the length of the intrusions with the initial height h_0, and included both the mixed solution initial condition (closed symbols) and the pure salt/pure sugar initial conditions (open symbols). Figure 11 shows the upper intrusion data, which seem to collapse so that L scales linearly with h_0. This agrees with the force balance argument given in (33). We have also included the average slope, or penetration velocity, of the experiments for both initial conditions. The velocity of the pure solutions is approximately three times larger than the mixed solutions. It is true that $\alpha\Delta T_0$ is three times larger for the pure solutions than for the mixed solutions, but from (33) we expect the velocity to vary like $(\alpha\Delta T_0)^{1/3}$. The data also collapses fairly well when we non-dimensionalize the length of the lower intrusion. The difference in velocities is more difficult to determine in this case due to the strong end wall effects.

7 Conclusions

We have attempted to show how horizontal thermohaline intrusions may develop because of vertical diffusion in a system stably stratified in both S and T. The problem was studied experimentally using sugar and salt solutions. We found that horizontal intrusions that lead to overturning in a layer initially of uniform density, but with horizontally varying concentrations of sugar and salt, can be driven purely by diffusion of the faster diffusing component from below. We also believe that the composition of this lower reservoir plays a large role in determining whether a diffusive or a fingering interface forms. This then in turn governs how sugar and salt are exchanged between the two upper layers. Further experiments will be carried out varying the reservoir concentrations to verify the importance of diffusion at this interface. Hopefully in future experiments we will be able to measure salt and sugar concentrations, which will provide information about the diffusive transfers across the interface and the evolution of the flux ratio. These experiments should offer helpful insights into the formation and mixing properties of thermohaline intrusions in regions such as the Southern Ocean.

Acknowledgments

I would like to thank all this summer's fellows and staff for providing an amazing environment in which to work. I take many valuable lessons from the lab, classroom and porch back with me. Special thanks go to Neil Balmforth for putting together a great program; Keith Bradley for assistance in the lab; Andy Woods for discussions that will hopefully extend beyond this summer; Julia, Chris, Anshuman and Amit for company in the lab and in the shack; and most importantly, George Veronis for his enthusiastic support and his patience throughout the summer (and for his confidence in me at SS in Phil's absence).

References

[1] O. M. Phillips B. R. Ruddick and J. S. Turner. A laboratory and quantitative model of finite-amplitude thermohaline intrusions. *Dyn. Atmos. Oceans*, 30:71–99, 1999.

[2] F. K. Browand and C. D. Winant. Blocking ahead of a cylinder moving in a stratified environment: An experiment. *Geophys. Fluid Dynamics*, 4:29–53, 1972.

[3] A. E. Gargett J. Tanny D. E. Kelley, H. J. S. Fernando and E. Ozsoy. The diffusive regime of double-diffusive convection. *Prog. in Oceanog.*, 56:461–481, 2003.

[4] H. Nagashima J. Yoshida and W. Ma. A double diffusive lock-exchange flow with small density difference. *Fluid Dynamics Res.*, 2:205–215, 1987.

[5] T. Maxworthy. The dynamics of double-diffusive gravity currents. *J. Fluid Mech.*, 128:259–282, 1983.

[6] B. Ruddick and O. Kerr. Oceanic thermohaline intrusions: theory. *Prog. in Oceanog.*, 56:483–497, 2003.

[7] B. R. Ruddick and T. G. L. Shirtcliffe. Data for double diffusers: Physical properties of aqueous salt–sugar solutions. *Deep-Sea Res.*, 26A:775–787, 1979.

[8] B. R. Ruddick and J. S. Turner. The vertical length scale of double-diffusive intrusions. *Deep-Sea Res.*, 26A:903–913, 1979.

[9] R. W. Schmitt. Double diffusion in oceanography. *Ann. Rev. Fluid Mech.*, 26:255–285, 1994.

[10] T. G. L. Shirtcliffe. Transport and profile measurements of the diffusive interface in double diffusive convection with similar diffusivities. *J. Fluid Mech.*, 57:27–43, 1973.

[11] M. E. Stern. Lateral mixing of water masses. *Deep-Sea Res.*, 14:747–753, 1967.

[12] W. Zenk T. M. Joyce and J. M. Toole. The anatomy of the antarctic polar front in the drake passage. *J. Geophys. Res.*, 83:6093–6113, 1978.

[13] J. S. Turner. *Buoyancy Effects in Fluids.* Cambridge University Press, Cambridge, 1973.

[14] D. Walsh and E. Carmack. A note on evanescent behavior of arctic thermohaline intrusions. *J. Mar. Res.*, 60:281–310, 2002.